東北大学機関リポジトリ
TOUR
Tohoku University Repository

Inverse tunnel magnetoresistance in magnetic tunnel junctions with as Fe#D4#DRN electrode

著者	角田　匡清
journal or publication title	Journal of applied physics
volume	102
number	1
page range	013917-1-013917-4
year	2007
URL	http://hdl.handle.net/10097/35040

doi: 10.1063/1.2753576

Inverse tunnel magnetoresistance in magnetic tunnel junctions with an Fe_4N electrode

Kazuyuki Sunaga and Masakiyo Tsunoda[a)]
Department of Electronic Engineering, Tohoku University, Aobayama 6-6-05, Sendai 980-8579, Japan

Kojiro Komagaki and Yuji Uehara
Advanced Head Technology Department, Fujitsu Ltd., Nagano 381-8501, Japan

Migaku Takahashi
New Industry Creation Hatchery Center, Tohoku University, Aobayama 6-6-10, Sendai 980-8579, Japan and Department of Electronic Engineering, Tohoku University, Aobayama 6-6-05, Sendai 980-8579, Japan

(Received 23 May 2007; accepted 29 May 2007; published online 13 July 2007)

The magnetotransport properties of $Fe_4N/MgO/CoFeB$ and Fe/MgO/CoFeB magnetic tunnel junctions (MTJs) were investigated at room temperature. In the Fe/MgO/CoFeB-MTJ, normal tunnel magnetoresistance (TMR) effect and roughly symmetric bias voltage (V_B) dependence were observed, similar to the MTJs exhibiting coherent tunneling such as Fe/MgO/Fe. On the other hand, the inverse TMR effect, showing higher tunnel resistance for parallel magnetization configuration than for antiparallel configuration, and strong asymmetric V_B dependence of TMR ratio were observed in the $Fe_4N/MgO/CoFeB$-MTJ. The maximum TMR magnitude of 18.5% was obtained at $V_B=-200$ mV, where the current flows from Fe_4N to CoFeB. The enhancement of the inverse TMR ratio around $V_B=-200$ mV is due to the broad peak of tunnel conductance in antiparallel configuration of Fe_4N and CoFeB magnetizations. A large peak of the density of state at +300 meV from the Fermi level for minority spin electrons of bulk Fe_4N might be an origin of this phenomenon. © *2007 American Institute of Physics*. [DOI: 10.1063/1.2753576]

I. INTRODUCTION

The giant tunnel magnetoresistance (TMR) effect was theoretically predicted[1–3] in MgO-based magnetic tunnel junctions (MTJs) and was experimentally confirmed[4,5] in fully epitaxial MTJs like as Fe(001)/MgO(001)/Fe(001). Furthermore, the experimental demonstration of a TMR ratio more than 200% at room temperature in sputter-deposited polycrystalline CoFeB/MgO/CoFeB MTJs,[6–10] accelerated the application development for the MgO-based MTJs, because of their suitability to mass production. In the CoFeB/MgO/CoFeB MTJs, amorphous CoFeB in the as-deposited state is crystallized with (001) out-of-plane texture during high temperature (>300 °C) annealing and results in the giant TMR ratio.[7,9,11] While the role of light element (boron) in these MTJs is known as an amorphous former in the metallurgical viewpoint, its role on the spin-polarized transport has not yet been fully understand. Nitrogen is a familiar light element, which forms various intermetallic compounds with 3*d*-transition metals and its role on the spin-polarized transport is also the subject to be studied. The Fe-N system shows a specific feature in its crystalline structure and resultant magnetic properties, as the N content is modified. Interstitially induced N atoms up to 12 at. % anisotropically expand the lattice of α-Fe and forms body-centered-tetragonal (bct) phase. Further doping of N up to 20 at. % in an octahedron site of Fe lattice transforms the bct structure to the face-centered-cubic structure and forms a thermodynamically stable γ'-Fe_4N phase. Therefore, the Fe-N system is suitable for examining the effect of a light element on the spin-polarized transport characteristic through the lattice distortion. In the present study, we employed γ'-Fe_4N as a first step of the studies for MgO-based MTJs with an Fe-N electrode and found a relatively large inverse TMR effect[12–14] at room temperature. The large inverse TMR effect is not only interesting from a physical viewpoint, but also useful for the application of MTJs especially for magnetic logic circuits to compose complementary switching elements with conventional normal TMR elements.

II. EXPERIMENTAL PROCEDURE

The specimens were deposited on thermally oxidized Si wafers with a design of substrate/under layer/bottom electrode / Mg(d_{Mg}) / MgO(2.0) / CoFeB(4) / Ru(0.9) / Fe(3) / $Mn_{73}Ir_{27}$(7.5) / Ta(5) / Ru(7) (thickness in nanometers) with using a magnetron sputtering system. During the deposition, the substrates were held at room temperature and a direct current (dc) magnetic field of 30 Oe was applied in the film plane. As a bottom electrode, either Fe_4N(50) or Fe(50) was employed with a MgO(2)/Fe(5) or MgO(5) under layer, respectively (thickness in nanometers). The Fe_4N layer was fabricated by dc reactive sputtering method from an Fe target, mixing N_2 gas into Ar. The MgO layer was deposited by radio frequency magnetron sputtering method from a sintered MgO target. The Mg layer inserted between the bottom electrode and the MgO barrier is aimed to prevent oxidation of the bottom electrode surface during the deposition of

[a)]Electronic mail: tsunoda@ecei.tohoku.ac.jp

 © 2007 American Institute of Physics

Downloaded 18 Aug 2008 to 130.34.135.158. Redistribution subject to AIP license or copyright; see http://jap.aip.org/jap/copyright.jsp

MgO barrier,[15,16] and its thickness, d_{Mg}, was 0.4 or 1.0 nm for the Fe_4N or Fe electrode, respectively. In order to improve the surface flatness of the bottom electrode, Fe_4N and Fe films were annealed at 350 and 250 °C, respectively, for 15 min, by using an infrared lamp heater, exposing their surface to vacuum less than 3×10^{-8} Torr, after the deposition without breaking vacuum. After cooling the specimen to room temperature, the remaining layers were deposited on it. The average surface roughness of the Fe_4N and Fe electrode was measured to be 0.13 and 0.36 nm, respectively, with using atomic force microscopy. A photolithographic process and ion milling were used to pattern the tunnel junctions in normal area of 64–6400 μm^2. The patterned Fe_4N- and Fe-MTJs were thermally annealed in vacuum at 320 and 400 °C for 1 h under an applied field of 3 kOe, respectively. Crystallographic structure was investigated for the sample wafers using x-ray diffraction (XRD) with a Cu $K\alpha$ radiation source. The preferred orientation of the MgO layer was determined from the integral intensity ratio of MgO(200) and MgO(220) diffraction lines, observed with the grazing incident x-ray diffraction method. When the MgO layer has (001) and (111) preferred orientations parallel to the film plane, the intensity ratio comes to be about 4 and 0, respectively. The magnetotransport properties were measured at room temperature with the dc four-probe method for the microfabricated MTJs. The magnetoresistance (MR) ratio was defined as $(R_{AP}-R_P)/R_P$, where R_P and R_{AP} are the tunneling resistances when the magnetizations of the two electrodes are aligned in parallel and antiparallel configuration, respectively.

III. RESULTS AND DISCUSSION

First, in order to fix a fabrication condition of the Fe_4N single phased electrode, Fe-N films were deposited with changing a N_2 mixing ratio to Ar and were characterized in their structure. Figure 1 shows XRD profiles for 50 nm thick Fe-N films on the MgO under layer as a function of the N_2 flow ratio to Ar. The thickness of the MgO under layer was fixed with 2 nm. The N_2 flow ratio was controlled from 0 to 34%. In the case of the Fe film fabricated in a pure Ar plasma, only a diffraction peak from the Fe(002) plane was observed around $2\theta=65°$, indicating a (001)-oriented single phase growth of Fe. The corresponding broad diffraction peak is observed around $2\theta=63.5°$ in the profile with increasing N_2 flow ratio from 0 to 2% but is shifted to the lower angle in 2θ. It means that the doped N atoms expand the *c* axis of Fe lattice. When the N_2 flow ratio was controlled with 20% and 25%, two diffraction lines are observed. These peaks are assigned to Fe(110) and $Fe_4N(002)$, respectively, referring the bulk lattice constants of them. It indicates a two-phase mixture state. However, when the N_2 flow ratio comes to be 30%, the Fe(110) diffraction line vanishes and only the $Fe_4N(002)$ peak remains. It means the (001)-oriented single-phase growth of Fe_4N. When the N_2 flow ratio exceeds 30%, the diffraction peak from Fe_3N appears at $2\theta=44°$, in contrast to before. Such a change of the crystallographic structure of the Fe-N film corresponds well with a phase diagram of the Fe-N system. The fabrication condition of the Fe_4N single phased film on the MgO under layer was thus fixed to a N_2 flow ratio of 30%.

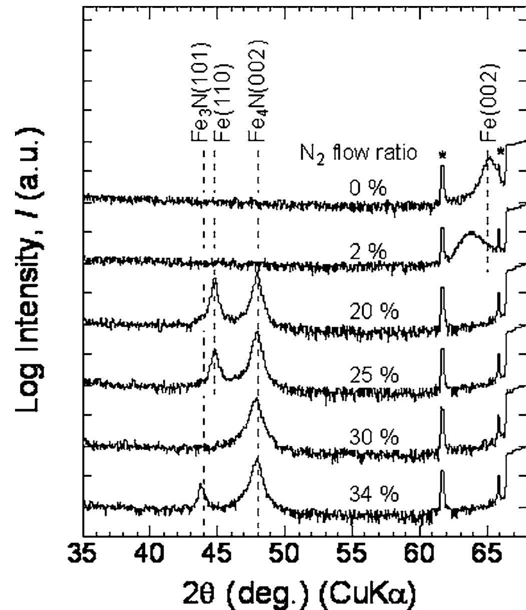

FIG. 1. XRD profiles for 50 nm thick Fe-N films with various N_2 flow ratio deposited on 2 nm thick MgO under layer. The peaks indexed with an asterisk are due to the substrate.

Figure 2 shows in-plane XRD profiles of MgO(2)/Fe(50)/MgO(10) and MgO(2)/Fe(5)/Fe_4N(50)/MgO(10) (thickness in nanometers) films. The incident angle of x rays was fixed at 0.1° and then the profiles reflect the structural information at a depth of approximately 10 nm from the film surface. In both cases, the MgO(200) and MgO(220) peaks were clearly observed. The integral intensity ratio of MgO(200) and MgO(220) diffraction lines was estimated as about 4 for both profiles. This means that the (001)-oriented

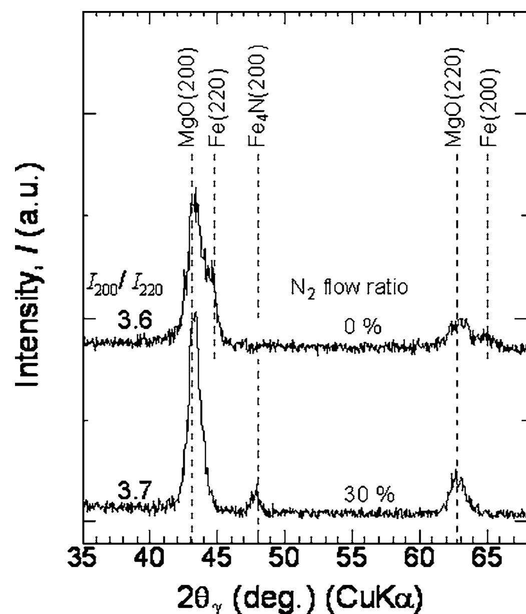

FIG. 2. In-plane XRD profiles of MgO(2)/Fe(50)/MgO(10) and MgO(2)/Fe(5)/Fe_4N(50)/MgO(10) (thickness in nanometers) films. Incident x-ray angle was fixed to 0.1°, thus the penetration depth is about 10 nm.

Downloaded 18 Aug 2008 to 130.34.135.158. Redistribution subject to AIP license or copyright; see http://jap.aip.org/jap/copyright.jsp

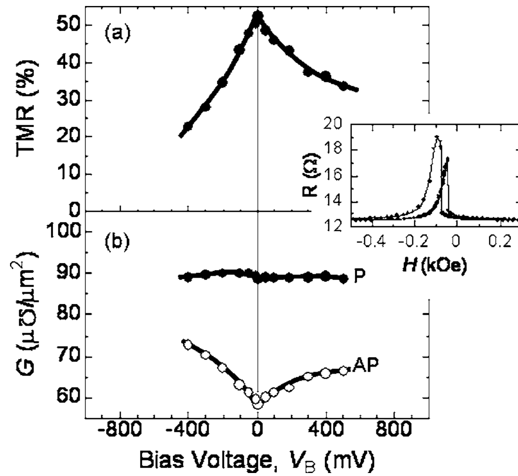

FIG. 3. Bias voltage dependence of (a) TMR ratio and (b) tunnel conductance at room temperature for the Fe/MgO/CoFeB MTJ. The conductance was measured for parallel (P) and antiparallel (AP) configuration of the Fe and CoFeB magnetizations. A positive bias voltage is defined as current from the upper CoFeB to the lower Fe electrode. Inset shows typical MR curve, measured at V_B=5 mV.

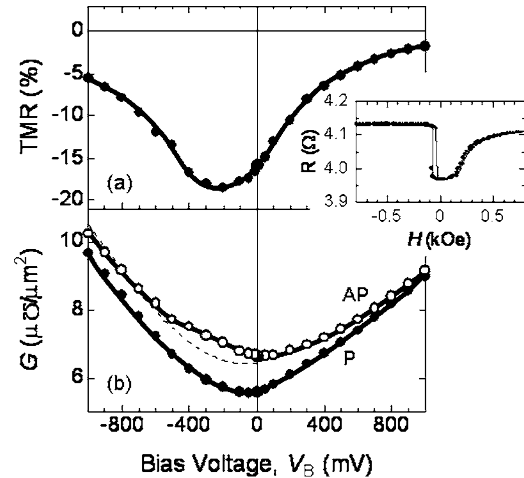

FIG. 4. Bias voltage dependence of (a) TMR ratio and (b) tunneling conductance at room temperature for the Fe_4N/MgO/CoFeB MTJ. A positive bias voltage is defined as current from the upper CoFeB to the lower Fe_4N electrode. Inset shows typical MR curve, measured at V_B=5 mV. The dashed line associated with antiparallel (AP) conductance is a guide for eyes showing a smooth trend curve, presumed from the curvature of the parallel (P) conductance.

MgO film on the Fe_4N or Fe layer was obtained. The lattice relationship between MgO, Fe, and Fe_4N films was then stated as MgO(001)//Fe(001)//MgO(001) and MgO(001)//Fe(001)//Fe_4N(001)//MgO(001).

Figure 3 shows the bias voltage (V_B) dependence of (a) the TMR and (b) the tunnel conductance per junction area, measured for the Fe/MgO/CoFeB MTJ. A positive bias voltage is defined to flow current from the upper electrode (CoFeB) to the lower electrode (Fe). The inset shows a typical MR curve, indicating normal-TMR effect. The maximum TMR ratio of about +50% was obtained around V_B=0. The conductance for the antiparallel (AP) configuration of Fe and CoFeB magnetizations increases as $|V_B|$ increases, while the conductance for the parallel (P) configuration is almost constant against V_B. This means that the V_B dependence of TMR ratio is mainly originated from the AP conductance. Taking into account that the flat response of the P conductance against V_B is commonly observed in MTJs with coherent tunneling mechanism,[17] we may say that the transport mechanism of the present Fe/MgO/CoFeB MTJ is coherent tunneling.

Figure 4 shows the bias voltage dependence of (a) the TMR and (b) the tunnel conductance per junction area, measured for the Fe_4N/MgO/CoFeB MTJ. The sign on bias voltage is defined as the same as Fig. 3. The typical TMR curve shown in the inset clearly demonstrates the inverse-TMR effect, where the P resistance is higher than the AP resistance. It implies that the spin polarization of the Fe_4N electrode has the opposite sign to that of the CoFeB electrode. The bias dependence of the TMR was not centered in zero bias and the maximum magnitude was obtained as 18.5% at V_B=−200 mV. The tunnel conductance in the parallel configuration is not flat against V_B, in contrast to the Fe-MTJ case, implying that the transport mechanism of the Fe_4N/MgO/CoFeB is not coherent tunneling. It takes the minimum around zero bias ($V_B \sim -50$ mV), differently from the TMR behavior. Namely, the asymmetry of the V_B dependence of TMR originates in the AP conductance. Here, we should notice that the AP conductance curve is not smooth in the negative voltage region. It inflects at both V_B=−500 mV and around V_B=0, and differs from the superimposed dashed line with a curvature of the P conductance. The most remarkable deviation of the AP conductance from the dashed curve is observed around V_B=−200 to −300 mV, corresponding with the peak of the inverse TMR ratio in Fig. 4(a). In other words, the AP conductance has a convex peak around V_B=−200 to −300 mV, and causes the concave shape of the TMR response to V_B. We will now consider the physical origin of the peak of AP conductance at that region, assuming the Julliere's model[18] and a positive sign of the spin polarization of CoFeB. As mentioned earlier, the transport mechanism of the Fe_4N-MTJ might not be the coherent tunneling and the spin polarization of the Fe_4N electrode is in opposite sign to that of CoFeB. Thus, the AP conductance in negative bias voltage reflects the density of state (DOS) for minority spin electrons of the Fe_4N electrode above the Fermi level. When we refer the calculated DOS of bulk Fe_4N, a large peak for the minority spin is found at +300 meV from the Fermi level.[19–21] The peak position of the minority spin DOS in electron energy is roughly corresponding with the peak position of the AP conductance in the bias voltage. Therefore, we may conclude that the inverse feature and the asymmetric V_B dependence of TMR are caused to the DOS of the Fe_4N electrode.

IV. SUMMARY

In summary, MTJs with Fe/MgO/CoFeB and Fe_4N/MgO/CoFeB structures were fabricated, and the magnetotransport properties were investigated at room temperature. In the Fe-MTJ, a normal TMR effect and roughly symmetric bias voltage (V_B) dependence were observed, similar to the MTJs exhibiting coherent tunneling such as Fe/MgO/Fe. On the other hand, in the Fe_4N-MTJ, an inverse TMR

Downloaded 18 Aug 2008 to 130.34.135.158. Redistribution subject to AIP license or copyright; see http://jap.aip.org/jap/copyright.jsp

effect and strong asymmetric V_B dependences were observed in the TMR ratio and tunnel conductance. The maximum TMR magnitude of 18.5% was obtained at $V_B=-200$ mV, where the current flows from Fe_4N to CoFeB. The enhancement of the inverse TMR ratio around $V_B=-200$ mV is due to the broad peak of tunnel conductance in antiparallel configuration of Fe_4N and CoFeB magnetization. A large peak of the density of state at +300 meV from the Fermi level for minority spin electrons of bulk Fe_4N might be an origin of this phenomenon.

[1] W. H. Butler, X.-G. Zhang, T. C. Schulthess, and J. M. MacLaren, Phys. Rev. B **63**, 054416 (2001).
[2] J. Mathon and A. Umersky, Phys. Rev. B **63**, 220403 (2001).
[3] X.-G. Zhang and W. H. Butler, Phys. Rev. B **70**, 172407 (2004).
[4] S. Yuasa, T. Nagahama, A. Fukushima, Y. Suzuki, and K. Ando, Nat. Mater. **3**, 868 (2004).
[5] S. S. Parkin, C. Kaiser, A. Panchula, P. M. Rice, B. Hughes, M. Samant, and S.-H. Yang, Nat. Mater. **3**, 862 (2004).
[6] D. D. Djayaprawira, K. Tsunekawa, M. Nagai, H. Maehara, S. Yamagata, N. Watanabe, S. Yuasa, Y. Suzuki, and K. Ando, Appl. Phys. Lett. **86**, 092502 (2005).
[7] J. Hayakawa, S. Ikeda, F. Matsukura, H. Takahashi, and H. Ohno, Jpn. J. Appl. Phys., Part 2 **44**, L587 (2005).
[8] S. Ikeda, J. Hayakawa, Y.-M. Lee, R. Sakai, T. Meguro, F. Matsukura, and H. Ohno, Jpn. J. Appl. Phys., Part 2 **44**, L1442 (2005).
[9] Y. M. Lee, J. Hayakawa, S. Ikeda, F. Matsukura, and H. Ohno, Appl. Phys. Lett. **89**, 042506 (2006).
[10] J. Hayakawa, S. Ikeda, Y. M. Lee, F. Matsukura, and H. Ohno, Appl. Phys. Lett. **89**, 232510 (2006).
[11] S. Yuasa, Y. Suzuki, T. Katayama, and K. Ando, Appl. Phys. Lett. **87**, 242503 (2005).
[12] J. M. De Teresa, A. Barthélémy, A. Fert, J. P. Contour, R. Lyonnet, F. Montaigne, P. Seneor, and A. Vaurès, Phys. Rev. Lett. **82**, 4288 (1999).
[13] C. Tiusan, M. Sicot, M. Hehn, C. Belouard, S. Andrieu, F. Montaigne, and A. Schuhl, Appl. Phys. Lett. **88**, 062512 (2006).
[14] C. Kaiser and S. S. P. Parkin, Appl. Phys. Lett. **88**, 112511 (2006).
[15] T. Lin and D. Mauri, US Patent No. 6,841,395 B2 (2005).
[16] K. Tsunekawa, D. D. Djayaprawira, M. Nagai, H. Maehara, S. Yuasa, Y. Suzuki, and K. Ando, Appl. Phys. Lett. **87**, 072503 (2005).
[17] C. Tiusan, M. Sicot, J. Faure-Vincent, M. Hehn, C. Bellouard, F. Montaigne, S. Andrieu, and A. Schuhl, J. Phys.: Condens. Matter **18**, 941 (2006).
[18] M. Julliere, Phys. Lett. **54A**, 225 (1975).
[19] A. Sakuma, J. Phys. Soc. Jpn. **60**, 2007 (1991).
[20] A. Sakuma, J. Magn. Magn. Mater. **102**, 127 (1991).
[21] S. Kokado, N. Fujima, K. Harigaya, H. Shimizu, and A. Sakuma, Phys. Rev. B **73**, 172410 (2006).

Downloaded 18 Aug 2008 to 130.34.135.158. Redistribution subject to AIP license or copyright; see http://jap.aip.org/jap/copyright.jsp